World Journal of Gastrointestinal Endoscopy

Online Submissions: http://www.wjgnet.com/esps/
bpgoffice@wjgnet.com
doi:10.4253/wjge.v5.i11.540

World J Gastrointest Endosc 2013 November 16; 5(11): 540-550
ISSN 1948-5190 (online)

MINIREVIEWS

Imaging pancreatobiliary ductal system with optical coherence tomography: A review

Mohammad S Mahmud, Gray R May, Mohammad M Kamal, Ahmed S Khwaja, Carry Sun, Alex Vitkin, Victor XD Yang

Mohammad S Mahmud, Carry Sun, Victor XD Yang, Department of Electrical and Computer Engineering, Biophotonics and Bioengineering Lab, Ryerson University, Toronto, M5B 2K3, Canada
Ahmed S Khwaja, Department of Electrical and Computer Engineering, Ryerson University, Toronto, M5B 2K3, Canada
Gray R May, Division of Gastroenterology, Saint Michael's Hospital, University of Toronto, Toronto, M5B 1W8, Canada
Mohammad M Kamal, Department of Burn and Plastic Surgery, Dhaka Medical College, Dhaka 1200, Bangladesh
Alex Vitkin, Department of Medical Biophysics, University of Toronto, Ontario Cancer Institute/University Health Network, Toronto, M5G 2M9, Canada
Author contributions: Mahmud MS prepared the article; May GR and Kamal MM provided technical supports during the study; Khwaja AS, Sun C and Vitkin A reviewed the manuscript; Yang VXD provided support of finance.
Correspondence to: Mohammad S Mahmud, PhD, Department of Electrical and Computer Engineering, Biophotonics and Bioengineering Lab, Ryerson University, 350 Victoria Street, Toronto, M5B 2K3, Canada. ssujann1@gmail.com
Telephone: +1-647-8854428 Fax: +1-416-9795280
Received: May 28, 2013 Revised: September 23, 2013
Accepted: October 15, 2013
Published online: November 16, 2013

Abstract

An accurate, noninvasive and cost-effective method of *in situ* tissue evaluation during endoscopy would be highly advantageous for the detection of dysplasia or early cancer and for identifying different disease stages. Optical coherence tomography (OCT) is a noninvasive, high-resolution (1-10 μm) emerging optical imaging method with potential for identifying microscopic subsurface features in the pancreatic and biliary ductal system. Tissue microstructure of pancreaticobiliary ductal system has been successfully imaged by inserting an OCT probe through a standard endoscope operative channel. High-resolution OCT images and the technique's endoscopic compatibility have allowed for the microstructural diagnostic of the pancreatobiliary diseases. In this review, we discussed currently available pancreaticobiliary ductal imaging systems to assess the pancreatobiliary tissue microstructure and to evaluate varieties of pancreaticobiliary disorders and diseases. Results show that OCT can improve the quality of images of pancreatobiliary system during endoscopic retrograde cholangiopancheatography procedure, which may be important in distinguishing between the neoplastic and non-neoplastic lesions.

Key words: Optical coherence tomography; Endoscopy; Common bile duct; Main pancreatic duct; Sphincter of Oddi; Benign and malignant strictures

Core tip: Optical coherence tomography is a high-resolution diagnostic tool for pancreatobiliary system during endoscopic retrograde cholangiopancheatography procedure.

Mahmud MS, May GR, Kamal MM, Khwaja AS, Sun C, Vitkin A, Yang VXD. Imaging pancreatobiliary ductal system with optical coherence tomography: A review. *World J Gastrointest Endosc* 2013; 5(11): 540-550 Available from: URL: http://www.wjgnet.com/1948-5190/full/v5/i11/540.htm DOI: http://dx.doi.org/10.4253/wjge.v5.i11.540

INTRODUCTION

Outstand from various existing diagnosis methods such as, endoscopic retrograde cholangiopancheatography (ERCP), percutaneous transhepatic cholangiography (PTC), magnetic resonance cholangiopancreatography (MRCP), computed tomographic cholangiography (CTC), endoscopic ultrasound guided fine-needle aspiration (EUS-FNA), available for the assessment of pancreatic

Table 1 Imaging methods for diagnosis of bile duct strictures *n* (%)

Techniques	SEN (%)	SPEC	PPV	NPV	Accuracy
BC/FNA[2,11,23]	30 (30-60)	95 (90-100)	100 (90-100)	28 (28-50)	48 (30-50)
Forceps biopsy[2,11,23]	43 (40-70)	90 (90-100)	95 (90-100)	31 (30-50)	48 (30-70)
BC + FNA + biopsy[2,11,23]	62 (60-75)	90 (90-100)	96 (90-100)	39 (35-60)	55 (45-75)
ERCP/MRCP[9,17,32,50-52]	70 (67-90)	75 (70-80)	80 (68-90)	88 (70-95)	70 (50-80)
ERCP-BC/BX[9,11,33,38]	43 (36-60)	80 (75-100)	95 (94-100)	90 (56-100)	70 (60-75)
EUS[17,32,33,47,53]	80 (70-100)	80 (75-100)	80 (76-100)	80 (54-90)	80 (78-90)
EUS-FNA[9,23]	85 (80-100)	95 (90-100)	95 (95-100)	80 (60-90)	85 (80-90)
IDUS[32,38]	90 (85-100)	85 (80-100)	85 (80-100)	90 (80-100)	90 (83-90)
IDUS + ERCP/biopsy[32,33,38,54]	91 (90-100)	93 (90-100)	94 (84-100)	90 (84-95)	92 (90-100)
OCT[1,2]	79 (75-90)	69 (65-90)	75 (70-90)	73 (70-90)	74 (70-85)
OCT-BC/BX[2]	84 (80-90)	69 (70-90)	76 (70-90)	78 (70-100)	77 (70-90)

True positive (TP) and true negative (TN) represent the accurate diagnosis of biliary and non-biliary strictures respectively; False positive (FP) reflects the incorrect diagnosis of non-malignancy, whereas, false negative (FN) reflects incorrect diagnosis of the benign strictures; Sensitivity, specificity, positive predictive values and negative predictive values were calculated as Ref. [54]. BC: Brush cytology; BX: Forceps biopsy; FNA: Fine-needle aspiration; ERCP: Endoscopic retrograde cholangiopancheatography; MRCP: Magnetic resonance cholangiopancreatography; EUS-FNA: Endoscopic ultrasound-guided FNA biopsy; IDUS: Intraductal ultrasonography; OCT: Optical coherence tomography; SEN: TP (TP + FN); SPEC: TN/(TN + FP); PPV: TP/(TP + FP); NPV: TN/(TN + FN).

and biliary disorders; optical coherence tomography (OCT) shows great potential for identifying dysplastic or early malignant epithelial changes and for differentiating between neoplastic and non-neoplastic lesions[1,2]. This is because ERCP and PTC are not risk free and in some cases, patients must undergo subsequent surgical or percutaneous procedures[3-5]. Additionally, diagnosis accuracy of ERCP-based tissue sampling (brush cytology and/or forceps biopsy) is relatively low (less than 70%) and highly variable[6-11]. Sometimes, tissue specimens collected with forceps biopsy and/or brushes may contain superficial tissue layers that are inherently insensitive to diagnosis and prone to false-negative results. MRCP[12-16] method is noninvasive, and is apparently less operator-dependent and its diagnostic accuracy is comparable (or slightly less) to ERCP. However, MRCP is expensive which requires additional tests for data analysis and diagnose diseases. Computed tomography[15-18] may provide better diagnostic information, but usually should be avoided due to the radiation exposures and contrast materials.

EUS-FNA is used for diagnosing cholangiocarcinoma and/or tumors in the biliary duct, especially in patients with negative brush cytology and forceps biopsy findings[19-27]. The technique shows diagnosis accuracy over 80%, however, the performance is hindered by system resolution; additionally expensive equipments are required during procedure. Intraductal ultrasonography (IDUS) is another safe and effective method performed during ERCP to diagnose localized stenosis and early malignant changes in main pancreatic duct[28,29], common bile duct stone[30,31] and to identify malignant biliary strictures[32-39]. During IDUS, a high-frequency ultrasound probe is placed into the pancreaticobiliary duct under ERCP guidance. IDUS shows diagnosis accuracy over 90% in patients with biliary strictures[31-38]. The major drawbacks of IDUS are the impossibility of tissue sampling and IDUS findings that might have showed limited reproducibility[30]. Therefore, more reliable and adequately sensitive diagnostic procedure is on demand for early detection of pancreatic and biliary diseases.

OCT an optical modality shows great potential for identifying dysplastic or early malignant epithelial changes and for differential diagnosis between neoplastic and non-neoplastic lesions. OCT is a noninvasive, high-resolution, cross-sectional *in vivo* imaging method based on the principle of low-coherence interferometry[40,41]. This technology has been widely used in various clinical and pathological applications, such as, in the field of ophthalmology[40,42], cardiology[43], gastroenterology[44,45], oncology[46], respiratory airways[47,48] and oral cavity disorder[49]. Main limitation OCT is its shallow penetration depth (2-3 mm) of imaging which depends upon the tissue structure, depth of focus of the probe used and absorption and/or scattering properties of the tissue sample.

General criteria (accuracy, sensitivity and specificity, positive and negative predictive values) of various imaging methods used to diagnose biliary duct strictures (malignant and benign) are summarized in Table 1. The advantages and disadvantages of these imaging modalities are listed in Table 2.

In this review, we focused on the feasibility of OCT approach that improves the diagnostic accuracy of the ductal epithelial changes, with a potential to diagnose neoplastic and non-neoplastic lesions as well as pancreatic cysts. We discussed the mechanism of an OCT imaging system and then image pancreatobiliary ductal system with OCT. The images of pancreaticobiliary ductal system are divided into two categories: normal pancreatico-biliary ductal system and pathological (neoplastic) ductal structure. Various pancreatic cysts with OCT are also discussed at the end of this review.

OCT IMAGING OF THE PANCREATOBILIARY DUCTAL SYSTEM

Introduction to OCT imaging system

Figure 1 shows the schematic diagram of an endoscopic

Table 2 Comparison of various imaging modalities

Imaging modality	PTC	ERCP	MRCP	US/HFUS/EUS/IDUS	CT	OCT
Projection/ tomograph	Projection	Projection	Projection or tomographic	Tomographic	Tomographic	Projection or tomographic
Resolution	1-2 mm	1-2 mm	Fairly poor 3-5 mm	US/EUS 100-250 μm HFUS/IDUS 50-100 μm	300-500 μm μCT: 3-125 μm	Fairly high 1-10 μm
Imaging depth	1-5 mm	5-60 mm	Entire biliary tree	US/EUS: 5-10 cm HFUS/IDUS: 1-3 cm	Entire biliary tree	1-3 mm
Tissue sampling	+ +	+ + +	-	US + EUS + + +	+	-
Portability	-	+	-	US + + + EUS + +	-	+ +
Therapy	+ + +	+ + +	-	US - EUS +	-	+
System cost	+ +	+ + + +	+ + +	US - EUS + +	+ +	+ +
Operator dependence	High	High	Low	Very high	Low	Low
Staging of malignancy	-	-	+ +	US + EUS + + +	+ + +	-
Safety	-	+	+ + +	+ +	+ +	+++
Experiment duration	2-4 h	30-120 min	10-30 min	20-40 min	15-30 s	5-10 min
Complications	+ + + Risk (5%-10%) of Infection, bleeding and bile leaks	+ + Risk (< 5%) Bleeding, perforationpancreatitis cholangitis	- Claustrophobia in some patients	+ Risk (1%) of failure rate, bleeding and perforation	- Rare allergic reaction (< 1%) to iodinated agents	- No complication
Comments pros	+ Diagnosis and therapeutic (treatment) procedure	+ Diagnosis and treatment procedure	Non-invasive + No ionizing radiation + Relatively operator -independent	Usually non-invasive (sedation) + Diagnosis tool combined with tissue and/or lesion sampling	Non-invasive + Faster method + High resolution + Operator-independent	Non-invasive + No ionizing radiation + High resolution + Faster method + Operator-independent
Cons	Invasive ionizing radiation Operator- dependent	Invasive Ionizing radiation Operator dependent	Expensive-poor resolution Solely diagnostic method Motion sensitive claustrophobia	Operator dependent Highly motion sensitive Thermal effects and cavitations	Ionizing radiation Solely diagnostic method	Low imaging depth 3 mm Motion sensitive

PTC: Percutaneous transhepatic cholangiography; ERCP: Endoscopic retrograde cholangiopancheatography; MRCP: Magnetic resonance cholangiopancreatography; US: Ultrasound; EUS: Endoscopic ultrasound; HFUS: High frequency ultrasound (> 10 MHz); IDUS: Intraductal ultrasonography; CT: Computed tomography; OCT: Optical coherence tomography.

OCT system. Light generated from a low coherence infrared light source spits into two parts: the sample and reference arms. The back-reflected light from the tissue interferes with the reference signal which then fed to a detector and then sent the signal to a computer for visualization. OCT is analogous to the ultrasound imaging[1], but uses light waves rather than ultrasound waves. Therefore, OCT provides high resolution (1-10 μm) which is at-least ten times better than the currently available high-frequency ultrasound imaging system. For investigating the epithelial layers of the main pancreatic duct (MPD), common bile duct (CBD) and sphincter of Oddi (SOD) an OCT probe (guide wire) is inserted through the working channel of an endoscopic catheter (Figure 1). The outer diameter of this endoscopic catheter can be made as small as 1.2 mm. Repeated frames are taken by the "pull-back" technique while connecting the catheter with a rotator, giving a large number of transitional-rotational images. Diagnoses of the intraductal pathology of the pancreatobiliary system, such as biliary and/or pancreatic stricture, are improved with OCT method where the conventional biopsy is technically difficult and is associated with risk[6,7]. After the targeted tissue is identified with a conventional endoscopy, a narrow-diameter (about 1.2 mm) OCT probe is inserted through the operating channel of the endoscope and positioned on the site of interest. No special patient preparation is required during OCT imaging and images can be acquired within several minutes (5-10 min). Three different types of OCT systems are wildly used in various research and clinical applications (Table 3). Companies currently produce OCT systems are: Novacam, Bioptigen, Heidelberg Engineering, Alcon/LenSx, Canon/Optopol, Volcano Crop, Optovue, Thorlabs, Topcon, Imalux, Nidek, Tomey, Schwind, Wasatchphotonics, OptiMedica, Optos/OTI, Volcano Crop, LightLab Imaging, Shenzhen Moptim Imaging, Techno-

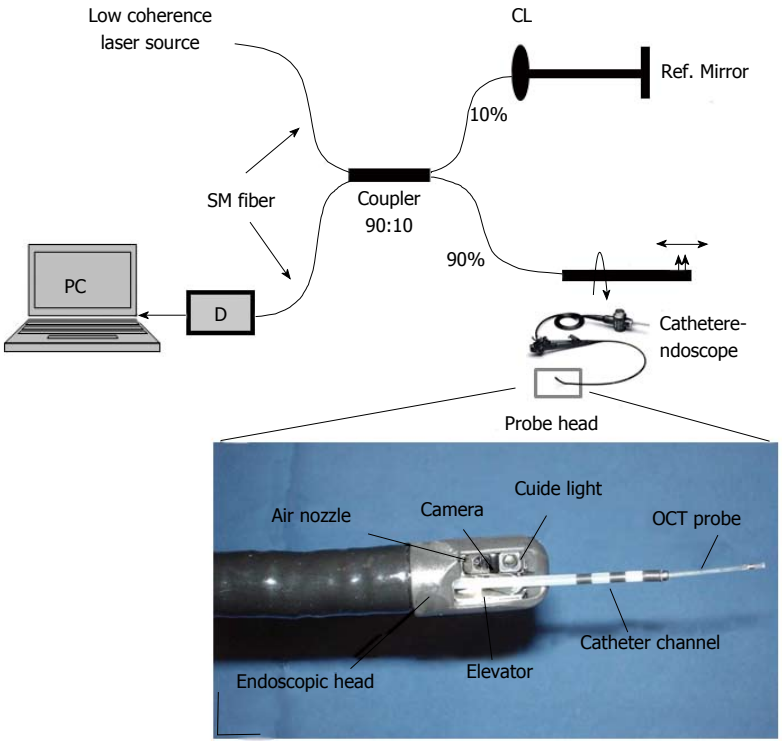

Figure 1 Schematic diagram of an endoscopic optical coherence tomography system. The endoscopic probe is connected to the sample arm (Color online). Light generated from a low coherence laser source spits into two parts, the sample arm and reference arm. Both back-reflected lights from sample and reference arms recombine in a fiber coupler (10:90). If both back-reflected reference and sample light travels the same distance (optical) then interference will occur and the interference signal will fed to a detector (D). Magnified region of interest in the second image is the endoscopic probe head, consisting primarily of an optical fiber (OCT probe), catheter channel, elevator, video camera and aiming light[55]. Scale bar: 10 mm.

Table 3 Comparison of different types of optical coherence tomography systems

Parameters	TD-OCT	SD-OCT	SS-OCT/OFDI
Mechanism	Interference signals are detected as a function of optical time delay between obj. and ref. arm.	Interference signals are detected with a camera as a function of optical frequency	Spectral fringes are mapped to time domain by use of a swept laser and are measured with a detector as a function of time
Major components	Broadband laser, optical delay line and a detector	Broadband laser, spectrometer and camera	Tunable laser, digitizer and a balanced detector
Spectrum	800 nm, 1000 nm, 1300 nm	800 nm, 1000 nm, 1300 nm	800 nm, 1000 nm, 1300 nm
Imaging depth	1-3 mm	1-3 mm	1-3 mm
Resolution	≥ 10 μm	1-10 μm	1-10 μm
Imaging speed (axial scan rate)	Slow (≤ 5 kHz)	Fast (20-150 kHz)	Fairly fast (20-400 kHz)
SNR	Low	High	High
Image quality	Moderate	Fairly high	High
Sensitivity	Low (70-90 dB)	High (85-105 dB)	High (≥ 100 dB)
Phase stability	Low	High	Moderate
Portability	Yes	Yes	Yes
System cost	Low	High	Moderate

SNR: Signal-to-noise ratio; dB: Decibel; TD-OCT: Time domain OCT; SD-OCT: Spectral-domain OCT; ODFI: Optical frequency domain imaging; SS-OCT: Swept source OCT.

las Perfect Vision, and Carl Zeiss Meditec. Cost of an OCT system varies with imaging engines (consisting of an interferometer, light source, and detector) and imaging devices (or OCT probes) and ranges from $20000-$80000. The cost per correct diagnosis (or procedure cost) is approximately $100 (100-200).

Normal pancreatobiliary ductal system

Visualization of epithelium layer structure of main pancreatic duct has been obtained from post-mortem[56] and *ex vivo* in humans[57-60], while *in vivo*, it comes from single study in animals[61] and another in humans[62]. Normal biliary ductal system was investigated in humans, *ex vivo* in a study[58,60], post-mortem[56] and *in vivo* and *ex vivo* in animals[61,63] and *in vivo* in ERCP-based OCT studies[2,64,65]. The SOD structure was investigated in normal and pathological conditions either in *ex vivo* or *in vivo* studies[2,58,65].

Human pancreatobiliary duct studies: Tearney *et al*[56] first performed *ex vivo* OCT imaging from the post-mortem cadaveric pancreatobiliary tissue. OCT images obtained from CBD-wall were able to identify layered structures and could resolve the submucosa-muscularis and muscularis-adventitia boundaries. Mucosa, submucosa, muscularis propria and adventitial layers, serosa in the gallbladder and biliary duct were visualized due to different back-

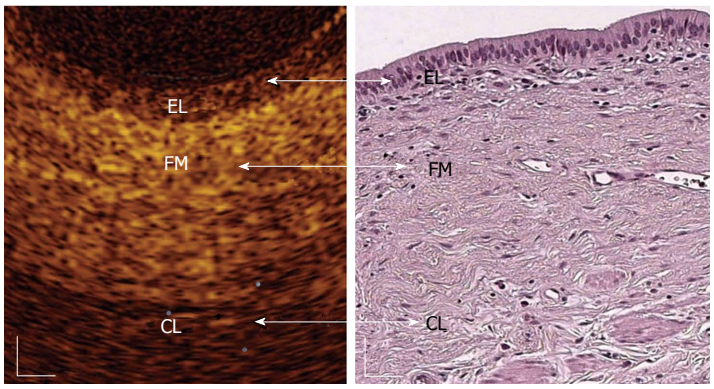

Figure 2 *In vivo* optical coherence tomography image of a normal common bile duct wall. Three recognizable layers were observed from the surface of the duct to a depth of 1 mm (Color online). The inner single layer of epithelial (EL) cells (400-600 μm thick) is visible as a superficial, hypo-reflective layer. The intermediate connective fibro-muscular (FM) layer surrounding the epithelium is visible as a hyper-reflective layer (350-480 μm thick) and the outer connective layer (CL) is visible as a hypo-reflective layer with longitudinal relatively hyper-reflective strips (smooth muscle fibers)[58]. White scale bar: 150 μm.

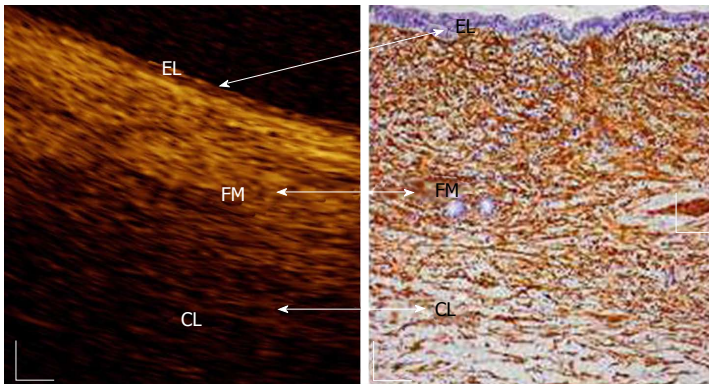

Figure 3 *In vivo* optical coherence tomography image of a normal main pancreatic duct wall compared with histology. Three recognizable layers were observed from the surface of the duct to a depth of 1 mm (Color online). The inner single layer of epithelial (EL) cells (400-800 μm thick) is visible as a superficial, hypo-reflective layer. The intermediate, connective fibro-muscular (FM) layer surrounding the epithelium, is visible as a hyper-reflective layer (350-600 μm thick). The outer connective-acinar (CL) structure close to the ductal wall epithelium is visible as a hypo-reflective layer[58]. White scale bar: 150 μm (right image).

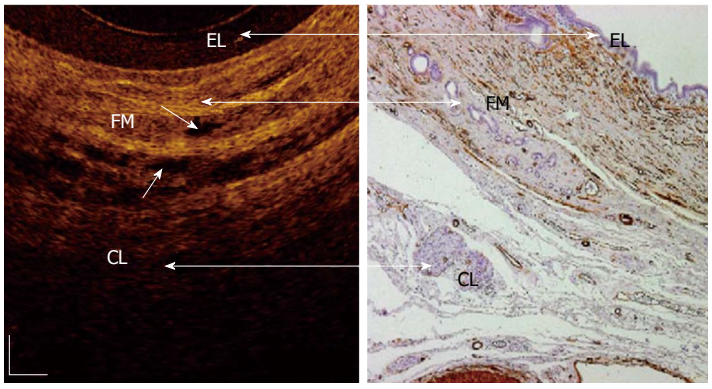

Figure 4 *In vivo* optical coherence tomography image of a normal sphincter of Oddi wall. Three recognizable layers were observed from the surface of the duct to a depth of 1 mm (Color online). The inner single layers of epithelial (EL) cells are visible as a superficial, hypo-reflective layer (400-800 μm thick). The intermediate connective-muscular (FM) layer surrounding the epithelium is visible as a hyper-reflective layer (250-400 μm thick). The outer connective layer (CL) is visible as a hypo-reflective layer with longitudinal relatively hyper-reflective strips (smooth muscle fibers). Within intermediate and outer layer, vessels could be visualized (marked with arrows) as nonreflecting areas. The boundaries between the intermediate and outer layers are not clearly recognizable due to irregular distribution of the connective and muscular structure[59]. White scale bar: 150 μm.

scattering characteristics within each layer. For example, submucosa and/or muscularis layers showed higher intensities and regular scattering pattern than the adventitial layer, most likely due to the presence of adipose tissue into the adventitial layer. The tissue microstructure, such as secretions within individual glands (glandular structure), and cross-sectional imaging of islets Langherans cells were visualized. The pancreatic duct appeared as a highly backscattering band near the lumen of the tissue and the pancreatic stroma was seen beneath the pancreatic duct.

Testoni *et al*[58,59,62,66] further studied *in vivo* MPD, CBD and SOD wall structures with OCT. Three different layers (Figures 2-4) were recognized from the surface of the duct to a depth of about 1 mm. The inner layer defined from the surface to the lumen, consisting of single layers of epithelial cells. The intermediate layer is homogeneous, consisting of connective fibro-muscular layer surrounding the epithelium. The outer layer is less definite and corresponds to the smooth muscular structure within a connective tissue in the CBD and at the level of the SOD, and connective-acinar structure in the MPD.

The inner hypo-reflective layer showed a mean thickness of 500 μm (range: 400-800 μm). Layer thickness, surface roughness and reflectance of inner layer were not substantially differing in CBD, MPD and SOD. Thickness of the intermediate hyper-reflective layer (about 400 μm) is substantially similar to MPD and CBD, whereas it reduces by 25% at the level of SOD[55]. Tiny, multiple, nonreflective areas can be appeared within the intermediate MPD layer and at the level of SOD (Figures 3 and 4). The outer hypo-reflective layer was recognizable up to a depth of about 1 mm (focus distance of the OCT probe) from the lumen. Multiple, smooth-muscle longitudinal strips appeared within hypo-reflective layer at the level of CBD and SOD and were particularly more

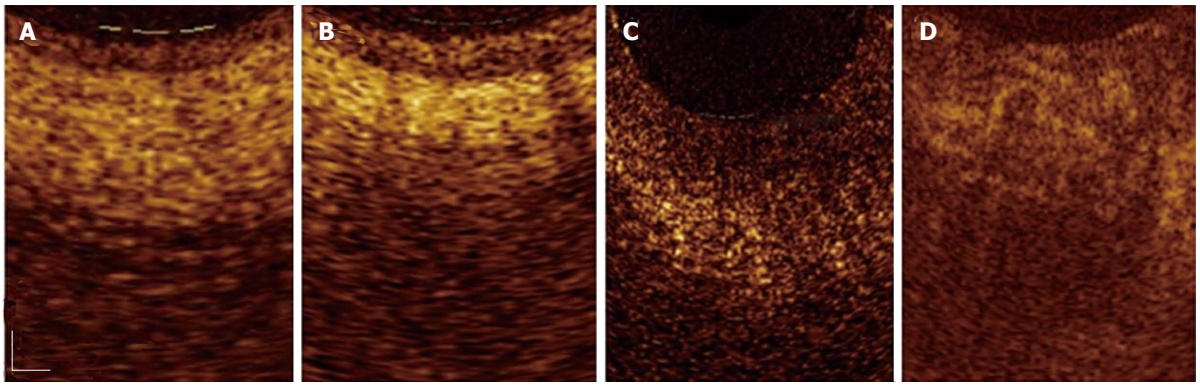

Figure 5 Magnified optical coherence tomography images. A: Sections with normal main pancreatic duct (MPD) wall; B: The presence of chronic pancreatitis; C: Low-grade dysplasia; D: Adenocarcinoma. Three differentiated layer architecture with a linear, regular surface, and a homogeneous back-scattered signal from each of the layer was observed in the normal condition. In the presence of chronic pancreatitis the optical coherence tomography (OCT) image still showed three-layer architecture, however, the inner epithelial layer appeared slightly larger than normal and the intermediate layer appeared more hyper-reflective; probably due to the presence of the dense mononuclear cell infiltrate. In the presence of dysplasia, OCT image showed thickened, strongly hypo-reflective and hetero-geneous inner MPD layer. Irregular surfaces were observed in the whole MPD structure. None of these layers were recognizable in the presence of adenocarcinoma[66]. Scale bar: 200 μm (Color online).

pronounced in SOD than in CBD. Furthermore, OCT images can identify veins, arteries and/or secondary pancreatic ducts which were characterized by hypo- or non-reflective, well delimited areas.

All of these layers showed linear, regular surface and each layer had a homogeneous back-scattered signal in every frame. However, the differentiation between outer and intermediate layer appeared more difficult than that of between inner and intermediate layer. The muscular and connective-acinar structure was visible until the focus distance (about 1 mm) of the OCT probe into the tissue.

Other biliary ductal studies: Singh *et al*[61] reported *in vivo* OCT images of animal (dog) pancreatic biliary ducts. Hwang *et al*[63] observed the normal structures of an *ex vivo* pig pancreas including small pancreatic ducts and pancreatic acini. OCT image identified biliary duct wall structure, features within lamina propria and some of the surrounding fibrous tissue. But OCT could not identify the nuclei or subcellular structures and/or adjacent structures such as blood vessels. A thin, low-scattering superficial layer appeared on the majority of the images, corresponding to the cuboidal epithelium. The lamina propria appeared as highly reflecting layer underneath the mucosal surface. Irregular reflections from layers underlying the lamina propria were from the dense connective tissue. Low reflected peribiliary glands were viewed as large open spaces with a single layer epithelium. The pancreatic duct in dogs has a flat mucosal layer composed of cuboidal epithelium and virtually has no lamina propria. OCT was able to image wall of the pancreatic duct but not the surrounding parenchyma. The pancreatic duct images were homogeneous and moderately reflective.

Pathological (dysplastic/neoplastic) pancreatobiliary ductal system

Imaging pathological pancreatic ductal system with OCT was first investigated by Testoni *et al*[59,60] in humans in two *ex vivo* studies. MPD chronic inflammatory changes showed a conserved, three-layer architecture. However, the inner hypo-reflective layer was slightly larger than the normal tissue layer and the intermediate layer was more hyper-reflective than normal condition. Additionally back-scattered signal from each layer is more heterogeneous than the normal layer condition.

In the presence of dysplasia, OCT showed thickened, strongly hypo-reflective and hetero-geneous inner layer of MPD (Figure 5C). Irregular surfaces were observed between the inner and intermediate layers. The intermediate layer is strongly hyper-reflectance, particularly close to the inner layer. The outer layer was homogeneously hypo-reflective and did not differ from normal condition. The agreement between OCT and histology in chronic pancreatitis and dysplasia were 62% in these cases. Overall, approximately one-third sections of normal wall structure and chronic inflammatory/low-grade dysplastic changes were not distinguishable with OCT.

In the presence of adenocarcinoma, MPD wall structure with OCT is shown in Figure 5D. All three layer structures and their linear, regular surface were not recognizable. No clear identifiable margin was seen between connective fibro-muscular layer and acinar tissue. The back-scattered signal was strongly heterogeneous with multiple nonreflective areas in the disorganized pancreatic microstructure. The OCT and histology were 100% concordant for sections with adenocarcinoma. OCT images from sections of MPD with normal tissue, tumor-associated chronic inflammation, low-grade dysplasia, and adenocarcinoma are shown in Figure 5.

OCT can differentiate three-layer architecture in either normal MPD or chronic pancreatitis; however, in a neoplastic lesion the layer architecture is totally subverted with heterogeneous light back-scattering. In addition, OCT can distinguish non-neoplastic from neoplastic lesions of MPD and can gave 100% accuracy for

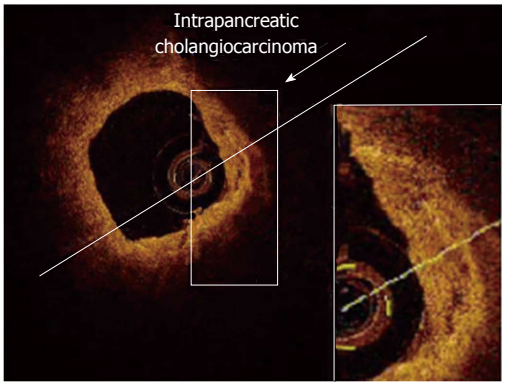

Figure 6 Adenocarcinoma (neoplasia) of the common bile duct at early stage, detected with optical coherence tomography probe maintained inside the endoscopic retrograde cholangiopancheatography catheter. In the presence of Adenocarcinoma (neoplasia), optical coherence tomography (OCT) patterns showed distorted common bile duct (CBD) wall structure (Color online). All three-layer architecture and their linear and regular surface, normally giving a homogeneous back-scattered signal, are not recognizable. OCT image shows heterogeneous back-scattered signal with minute, multiple, nonreflective areas (necrotic areas) in the highly disorganized CBD microstructure. Therefore, epithelial structure and various biliary disorders in early-stage of cancer can be distinguishable with OCT[67].

detection of neoplastic tissue compared with 66.7% for brush cytology[62]. MPD layer architectures derived from different back-scattered signals from each layer were confirmed as a reliable OCT parameter for distinguishing non-neoplastic from neoplastic tissue. However, this technology is unable to discriminate between a normal MPD structure and other MPD benign lesions. Further studies are necessary which might improve the diagnostic accuracy of OCT in this challenging imaging scenario.

OCT imaging during ERCP can identify CBD layer structure and diagnose neoplastic lesions and/or adenocarcinoma at early stages which is usually missed by cytology and X-ray imaging[55-67]. The normal CBD wall shows three recognizable layers, with a linear, regular surface and different homogeneous back-scattering of the light[58]. These inner to outer layers are: epithelium, connective-fibromuscular, and muscular layer in normal CBD wall (Figure 2). However, with the presence of neoplastic tissue, OCT patterns showed distorted CBD wall structure with heterogeneous light back-scattering (Figure 6). Therefore, epithelial structure and various biliary disorders in early-stage of cancer can be distinguishable with OCT.

Arvanitakis *et al*[2] conducted biliary intraductal OCT during ERCP studies in thirty-seven patients with biliary strictures and assess the potential of this method for improving the diagnosis accuracy of the malignant biliary strictures. This study concluded to satisfactory accuracy levels regarding distinction between malignant and benign strictures, especially when combined to biopsies. Based on OCT images, two malignancy criteria were considered: (1) disorganized and subverted layer architecture and (2) presence of large nonreflective areas compatible with tumor vessels. Figure 7A shows the cross-sectional OCT image of a patient with a benign stricture. The probe is surrounded by ERCP catheter (marked with arrow). The three-layered structure of the biliary wall is recognizable. Figure 7B-D show images of the malignant bile duct strictures. Disorganized layer architecture of the stricture wall which is one of the criteria for malignancy is shown in Figure 7B. Large, nonreflective, surface of at least 0.03 mm^2 tumor vessels were observed in Figure 7C. Malignant stricture due to hilar metastases of an esophageal squamous carcinoma was observed in Figure 7D.

Studies of pancreatic cysts with OCT

OCT modality shows great potential to reveal specific morphologic features of pancreatic cysts and thus to differentiate between the interior structures of low risk (*i.e.,* serous cyst adenomas) and high risk (*i.e.,* mucinous cystic neoplasms and intraductal papillary mucinous neoplasms) pancreatic cysts with over 95% sensitivity and specificity[68,69]. Fresh pancreatic specimens (pancreatic cysts) from patients were made available immediately after the surgery and then examined with OCT. An OCT probe was inserted into the cut surface of the pancreatic cysts. The main characteristics of each type of cystic lesion are shown in Figure 8.

Based on OCT images, the cysts were prospectively divided into two groups: mucinous (*i.e.,* Mucinous Cystic Neoplasms and Intraductal Papillary Mucinous Neoplasms) and non-mucinous (*i.e.,* Serous Cysts Adenomas and others). Multiple tiny cysts with well-defined outlines are seen in low-risk (*i.e.,* Serous Cysts Adenomas) of pancreatic cystic lesions. Thin septae between cysts create honeycomb appearance. The cyst content usually appears as dark due to lack of the scattering effect. Focal intra-luminal scattering can be found in some cysts which usually correspond to hemorrhage. In high-risk (*i.e.,* Mucinous Cystic Neoplasms, Intraductal Papillary Mucinous Neoplasms) pancreatic cyst multiple small cysts present (marked with white arrow), which may sometime surround the main cystic cavity (marked with red arrow). The cystic content may show some scattering due to presence of dead epithelial cells.

The above criteria mainly based on the visual appearance of the cystic wall morphology and on the scattering properties of the cystic fluid. Although relatively simple, they provide a very good discrimination between serous and mucinous pancreatic cysts. This *ex vivo* study suggests that OCT could be used by clinicians in future to more reliably differentiate between benign and malignant pancreatic cysts.

CONCLUSION

Limitations of standard endoscopic practices are addressed by the OCT technology described in this review. OCT identified layer structures of common bile duct, main pancreatic duct and sphincter of oddi and could resolve the submucosa-muscularis and muscularis-adven-

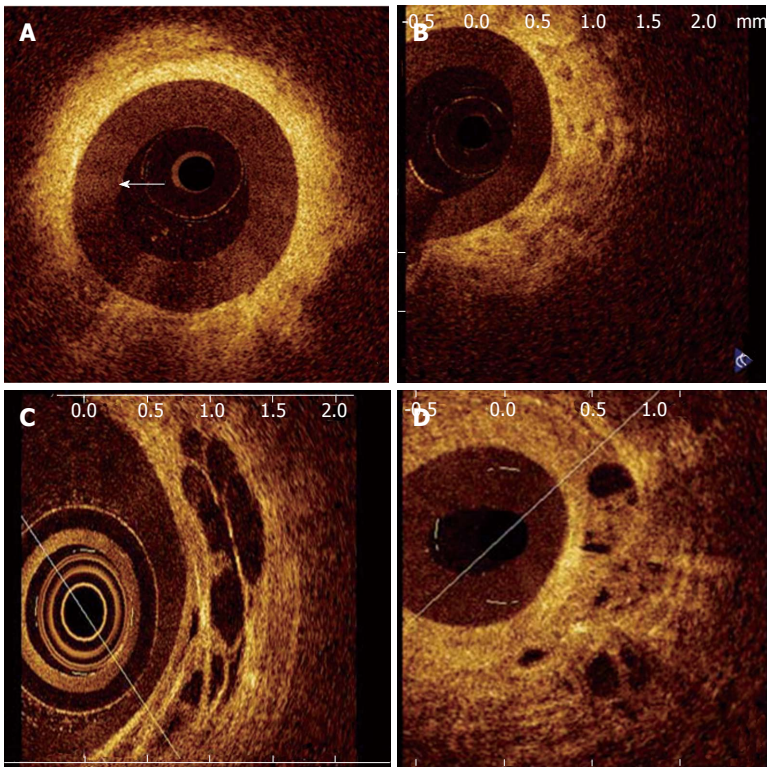

Figure 7 Optical coherence tomography image of a patient with a benign stricture. The three-layered structure of the biliary wall is recognizable (Color online). A-D shows images of malignant bile duct strictures. B: Disorganized layered structure with unidentifiable margins and a strongly heterogeneous backscattering signal; C: Large, nonreflective areas in the intermediate layer suggesting the tumor vessels; D: Malignant stricture due to hilar metastases of an esophageal squamous carcinoma showing nonreflective areas and disorganized layer architecture[2].

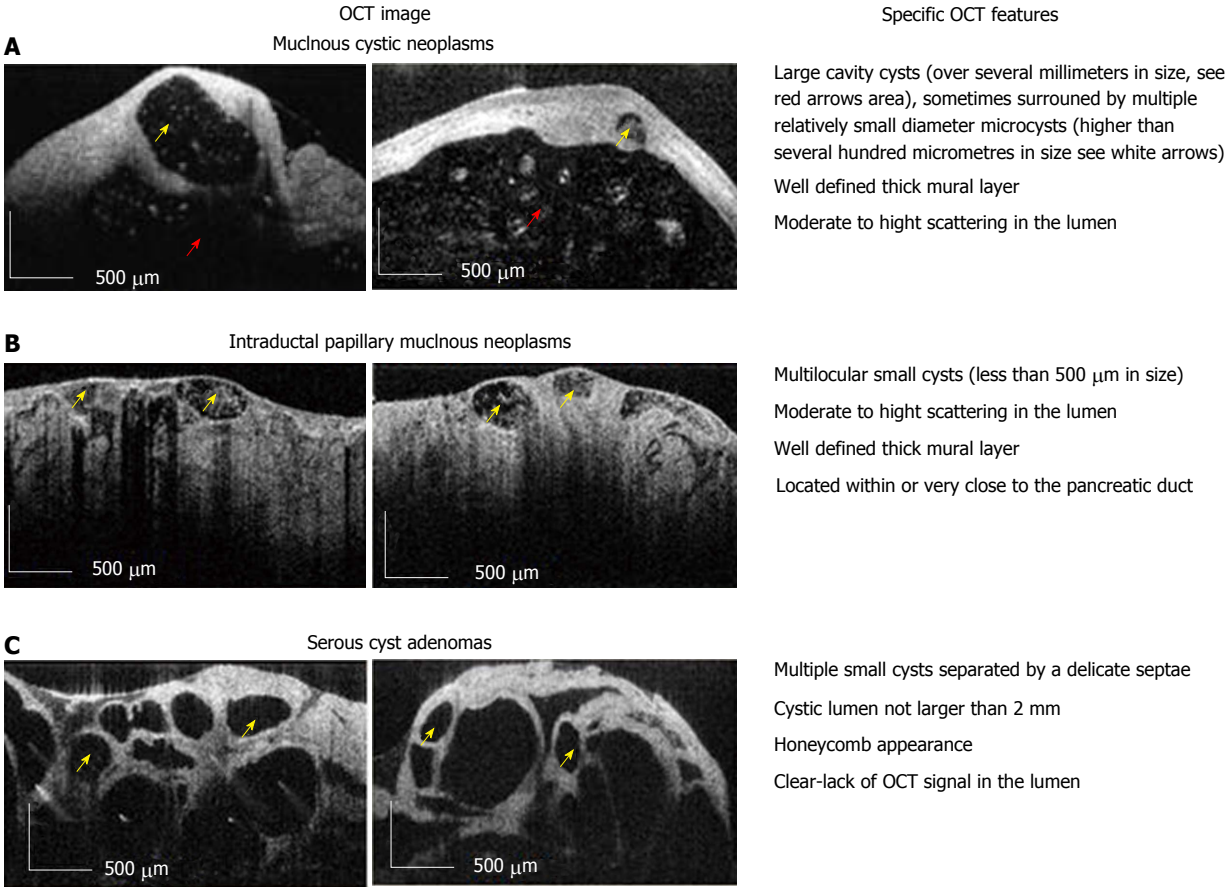

Figure 8 Optical coherence tomography image. A, B: Diagnostic criteria for high-risk (*i.e.*, Mucinous Cystic Neoplasms, Intraductal Papillary Mucinous Neoplasms); C: Low risk (*i.e.*, Serous Cysts Adenomas) pancreatic cysts. Multiple small cysts are marked with yellow arrow, while surrounded main cystic cavity is marked with red arrow. Scale bar = 500 μm[69]. OCT: Optical coherence tomography.

titia boundaries. Layers of these biliary ducts showed linear, homogeneous and regular surface; however, the difference between hypo-reflective intermediate and hypo-reflective outer layer appeared more difficult than that of between the hypo-reflective inner and intermediate layer. Potentially, OCT shows real-time, high-resolution, cross-sectional images, or "optical biopsies" for detecting the early stages of pancreatiobiliary diseases. OCT can improve the quality of images obtained during ERCP, which may be important in distinguishing between the neoplastic and non-neoplastic lesions. Further studies are necessary for the proper clinical applications of this promising method in the pancreaticobiliary duct system and diagnosis of pancreatic cysts.

ACKNOWLEDGMENTS

Authors thank Dr. Khwaja, Mr. Vuong, Dr. Cheng and Ms. Cirocco for their useful discussions. Authors thank Prof. Testoni (Vita-Salute San Raffaele Univ, Italy) for his permission to use the pancreatobiliary ductal endoscopic OCT images in this review.

REFERENCES

1 **Das A**, Sivak MV, Chak A, Wong RC, Westphal V, Rollins AM, Willis J, Isenberg G, Izatt JA. High-resolution endoscopic imaging of the GI tract: a comparative study of optical coherence tomography versus high-frequency catheter probe EUS. *Gastrointest Endosc* 2001; **54**: 219-224 [PMID: 11474394 DOI: 10.1067/mge.2001.116109]

2 **Arvanitakis M**, Hookey L, Tessier G, Demetter P, Nagy N, Stellke A, De Maertelaer V, Devière J, Le Moine O. Intraductal optical coherence tomography during endoscopic retrograde cholangiopancreatography for investigation of biliary strictures. *Endoscopy* 2009; **41**: 696-701 [PMID: 19618343 DOI: 10.1055/s-0029-1214950]

3 **Chen VK**, Arguedas MR, Kilgore ML, Eloubeidi MA. A cost-minimization analysis of alternative strategies in diagnosing pancreatic cancer. *Am J Gastroenterol* 2004; **99**: 2223-2234 [PMID: 15555006 DOI: 10.1111/j.1572-0241.2004.40042.x]

4 **Neuhaus H**, Feussner H, Ungeheuer A, Hoffmann W, Siewert JR, Classen M. Prospective evaluation of the use of endoscopic retrograde cholangiography prior to laparoscopic cholecystectomy. *Endoscopy* 1992; **24**: 745-749 [PMID: 1468389 DOI: 10.1055/s-2007-1010576]

5 **Zeman RK**, Burrell MI, Dobbins J, Jaffe MH, Choyke PL. Postcholecystectomy syndrome: evaluation using biliary scintigraphy and endoscopic retrograde cholangiopancreatography. *Radiology* 1985; **156**: 787-792 [PMID: 4023244]

6 **Vandervoort J**, Soetikno RM, Montes H, Lichtenstein DR, Van Dam J, Ruymann FW, Cibas ES, Carr-Locke DL. Accuracy and complication rate of brush cytology from bile duct versus pancreatic duct. *Gastrointest Endosc* 1999; **49**: 322-327 [PMID: 10049415 DOI: 10.1016/S0016-5107(99)70008-8]

7 **Selvaggi SM**. Biliary brushing cytology. *Cytopathology* 2004; **15**: 74-79 [PMID: 15056166 DOI: 10.1111/j.1365-2303.2004.00133.x]

8 **Pugliese V**, Pujic N, Saccomanno S, Gatteschi B, Pera C, Aste H, Ferrara GB, Nicolò G. Pancreatic intraductal sampling during ERCP in patients with chronic pancreatitis and pancreatic cancer: cytologic studies and k-ras-2 codon 12 molecular analysis in 47 cases. *Gastrointest Endosc* 2001; **54**: 595-599 [PMID: 11677475 DOI: 10.1067/mge.2001.119220]

9 **Rösch T**, Hofrichter K, Frimberger E, Meining A, Born P, Weigert N, Allescher HD, Classen M, Barbur M, Schenck U, Werner M. ERCP or EUS for tissue diagnosis of biliary strictures? A prospective comparative study. *Gastrointest Endosc* 2004; **60**: 390-396 [PMID: 15332029 DOI: 10.1016/S0016-5107(04)01732-8]

10 **de Groen PC**, Gores GJ, LaRusso NF, Gunderson LL, Nagorney DM. Biliary tract cancers. *N Engl J Med* 1999; **341**: 1368-1378 [PMID: 10536130]

11 **de Bellis M**, Sherman S, Fogel EL, Cramer H, Chappo J, McHenry L, Watkins JL, Lehman GA. Tissue sampling at ERCP in suspected malignant biliary strictures (Part 2). *Gastrointest Endosc* 2002; **56**: 720-730 [PMID: 12397282 DOI: 10.1067/mge.2002.129219]

12 **Georgopoulos SK**, Schwartz LH, Jarnagin WR, Gerdes H, Breite I, Fong Y, Blumgart LH, Kurtz RC. Comparison of magnetic resonance and endoscopic retrograde cholangiopancreatography in malignant pancreaticobiliary obstruction. *Arch Surg* 1999; **134**: 1002-1007 [PMID: 10487597 DOI: 10.1001/archsurg.134.9.1002]

13 **Fulcher AS**, Turner MA. Benign diseases of the biliary tract: evaluation with MR cholangiography. *Semin Ultrasound CT MR* 1999; **20**: 294-303 [PMID: 10527135 DOI: 10.1016/S0887-2171(99)90061-6]

14 **Hussain SZ**, Bloom DA, Tolia V. Caroli's disease diagnosed in a child by MRCP. *Clin Imaging* 2000; **24**: 289-291 [PMID: 11331159 DOI: 10.1016/S0899-7071(00)00215-1]

15 **Soto JA**. Bile duct stones: diagnosis with MR cholangiography and helical CT. *Semin Ultrasound CT MR* 1999; **20**: 304-316 [PMID: 10527136 DOI: 10.1016/S0887-2171(99)90062-8]

16 **Kinney TP**, Freeman ML. Pancreatic imaging: current state of the art. *Gastroenterology* 2009; **136**: 776-779 [PMID: 19168064 DOI: 10.1053/j.gastro.2009.01.023]

17 **Rösch T**, Meining A, Frühmorgen S, Zillinger C, Schusdziarra V, Hellerhoff K, Classen M, Helmberger H. A prospective comparison of the diagnostic accuracy of ERCP, MRCP, CT, and EUS in biliary strictures. *Gastrointest Endosc* 2002; **55**: 870-876 [PMID: 12024143 DOI: 10.1067/mge.2002.124206]

18 **Stabile Ianora AA**, Memeo M, Scardapane A, Rotondo A, Angelelli G. Oral contrast-enhanced three-dimensional helical-CT cholangiography: clinical applications. *Eur Radiol* 2003; **13**: 867-873 [PMID: 12664128 DOI: 10.1007/s00330-002-1536-6]

19 **Giovannini M**, Seitz JF, Monges G, Perrier H, Rabbia I. Fine-needle aspiration cytology guided by endoscopic ultrasonography: results in 141 patients. *Endoscopy* 1995; **27**: 171-177 [PMID: 7601050 DOI: 10.1055/s-2007-1005657]

20 **Anand D**, Barroeta JE, Gupta PK, Kochman M, Baloch ZW. Endoscopic ultrasound guided fine needle aspiration of non-pancreatic lesions: an institutional experience. *J Clin Pathol* 2007; **60**: 1254-1262 [PMID: 17220205 DOI: 10.1136/jcp.2006.045955]

21 **Erickson RA**. EUS-guided FNA. *Gastrointest Endosc* 2004; **60**: 267-279 [PMID: 15278063 DOI: 10.1016/S0016-5107(04)01529-9]

22 **Itoi T**, Itokawa F, Sofuni A, Kurihara T, Tsuchiya T, Ishii K, Tsuji S, Ikeuchi N, Moriyasu F. Endoscopic ultrasound-guided choledochoduodenostomy in patients with failed endoscopic retrograde cholangiopancreatography. *World J Gastroenterol* 2008; **14**: 6078-6082 [PMID: 18932289 DOI: 10.3748/wjg.14.6078]

23 **Ross WA**, Wasan SM, Evans DB, Wolff RA, Trapani LV, Staerkel GA, Prindiville T, Lee JH. Combined EUS with FNA and ERCP for the evaluation of patients with obstructive jaundice from presumed pancreatic malignancy. *Gastrointest Endosc* 2008; **68**: 461-466 [PMID: 18384788 DOI: 10.1016/j.gie.2007.11.033]

24 **Sakamoto H**, Kitano M, Kamata K, El-Masry M, Kudo M. Diagnosis of pancreatic tumors by endoscopic ultrasonography. *World J Radiol* 2010; **2**: 122-134 [PMID: 21160578 DOI: 10.4329/wjr.v2.i4.122]

25 **Lee KH**, Lee JK. Interventional endoscopic ultrasonography: present and future. *Clin Endosc* 2011; **44**: 6-12 [PMID: 22741106 DOI: 10.5946/ce.2011.44.1.6]

26 **Ranney N**, Phadnis M, Trevino J, Ramesh J, Wilcox CM, Varadarajulu S. Impact of biliary stents on EUS-guided FNA of pancreatic mass lesions. *Gastrointest Endosc* 2012; **76**: 76-83 [PMID: 22726468 DOI: 10.1016/j.gie.2012.02.049]

27 **Hewitt MJ**, McPhail MJ, Possamai L, Dhar A, Vlavianos P, Monahan KJ. EUS-guided FNA for diagnosis of solid pancreatic neoplasms: a meta-analysis. *Gastrointest Endosc* 2012; **75**: 319-331 [PMID: 22248600 DOI: 10.1016/j.gie.2011.08.049]

28 **Benson MD**, Gandhi MR. Ultrasound of the hepatobiliary-pancreatic system. *World J Surg* 2000; **24**: 166-170 [PMID: 10633143 DOI: 10.1007/s002689910029]

29 **Tanaka K**, Kida M. Role of endoscopy in screening of early pancreatic cancer and bile duct cancer. *Dig Endosc* 2009; **21** Suppl 1: S97-S100 [PMID: 19691747 DOI: 10.1111/j.1443-1661.2009.00856.x]

30 **Levy MJ**, Baron TH, Clayton AC, Enders FB, Gostout CJ, Halling KC, Kipp BR, Petersen BT, Roberts LR, Rumalla A, Sebo TJ, Topazian MD, Wiersema MJ, Gores GJ. Prospective evaluation of advanced molecular markers and imaging techniques in patients with indeterminate bile duct strictures. *Am J Gastroenterol* 2008; **103**: 1263-1273 [PMID: 18477350 DOI: 10.1111/j.1572-0241.2007.01776.x]

31 **Lu J**, Guo CY, Xu XF, Wang XP, Wan R. Efficacy of intraductal ultrasonography in the diagnosis of non-opaque choledocholith. *World J Gastroenterol* 2012; **18**: 275-278 [PMID: 22294831 DOI: 10.3748/wjg.v18.i3.275]

32 **Vazquez-Sequeiros E**, Baron TH, Clain JE, Gostout CJ, Norton ID, Petersen BT, Levy MJ, Jondal ML, Wiersema MJ. Evaluation of indeterminate bile duct strictures by intraductal US. *Gastrointest Endosc* 2002; **56**: 372-379 [PMID: 12196775 DOI: 10.1067/mge.2002.126907]

33 **Farrell RJ**, Agarwal B, Brandwein SL, Underhill J, Chuttani R, Pleskow DK. Intraductal US is a useful adjunct to ERCP for distinguishing malignant from benign biliary strictures. *Gastrointest Endosc* 2002; **56**: 681-687 [PMID: 12397276 DOI: 10.1067/mge.2002.128918]

34 **Tantau M**, Pop T, Badea R, Spirchez Z, Moşteanu O, Tantau A. Intraductal ultrasonography for the assessment of preoperative biliary and pancreatic strictures. *J Gastrointestin Liver Dis* 2008; **17**: 217-222 [PMID: 18568147]

35 **Tamada K**, Ushio J, Sugano K. Endoscopic diagnosis of extrahepatic bile duct carcinoma: Advances and current limitations. *World J Clin Oncol* 2011; **2**: 203-216 [PMID: 21611097 DOI: 10.5306/wjco.v2.i5.203]

36 **Tamada K**, Tomiyama T, Wada S, Ohashi A, Satoh Y, Ido K, Sugano K. Endoscopic transpapillary bile duct biopsy with the combination of intraductal ultrasonography in the diagnosis of biliary strictures. *Gut* 2002; **50**: 326-331 [PMID: 11839709 DOI: 10.1136/gut.50.3.326]

37 **Menzel J**, Poremba C, Dietl KH, Domschke W. Preoperative diagnosis of bile duct strictures--comparison of intraductal ultrasonography with conventional endosonography. *Scand J Gastroenterol* 2000; **35**: 77-82 [PMID: 10672839]

38 **Domagk D**, Poremba C, Dietl KH, Senninger N, Heinecke A, Domschke W, Menzel J. Endoscopic transpapillary biopsies and intraductal ultrasonography in the diagnostics of bile duct strictures: a prospective study. *Gut* 2002; **51**: 240-244 [PMID: 12117887]

39 **Kawashima H**, Hirooka Y, Itoh A, Hara K, Kanamori A, Uchida H, Goto J, Nonogaki K, Matsumoto Y, Ohmiya N, Niwa Y, Goto H. Progress of endoscopic ultrasonography and intraductal ultrasonography in the diagnosis of malignant biliary diseases. *J Hepatobiliary Pancreat Surg* 2006; **13**: 69-74 [PMID: 16547664 DOI: 10.1007/s00534-005-1060-6]

40 **Huang D**, Swanson EA, Lin CP, Schuman JS, Stinson WG, Chang W, Hee MR, Flotte T, Gregory K, Puliafito CA. Optical coherence tomography. *Science* 1991; **254**: 1178-1181 [PMID: 1957169 DOI: 10.1126/science.1957169]

41 **Fercher AF**. Optical coherence tomography - development, principles, applications. *Z Med Phys* 2010; **20**: 251-276 [PMID: 21134630 DOI: 10.1016/j.zemedi.2009.11.002]

42 **Srinivasan VJ**, Wojtkowski M, Witkin AJ, Duker JS, Ko TH, Carvalho M, Schuman JS, Kowalczyk A, Fujimoto JG. High-definition and 3-dimensional imaging of macular pathologies with high-speed ultrahigh-resolution optical coherence tomography. *Ophthalmology* 2006; **113**: 2054.e1-2054. e 14 [PMID: 17074565 DOI: 10.1016/j.ophtha.2006.05.046]

43 **Jang IK**, Tearney GJ, MacNeill B, Takano M, Moselewski F, Iftima N, Shishkov M, Houser S, Aretz HT, Halpern EF, Bouma BE. In vivo characterization of coronary atherosclerotic plaque by use of optical coherence tomography. *Circulation* 2005; **111**: 1551-1555 [PMID: 15781733 DOI: 10.1161/01.CIR.0000159354.43778.69]

44 **Zhang J**, Chen Z, Isenberg G. Gastrointestinal optical coherence tomography: clinical applications, limitations, and research priorities. *Gastrointest Endosc Clin N Am* 2009; **19**: 243-259 [PMID: 19423022 DOI: 10.1016/j.giec.2009.02.003]

45 **Evans JA**, Poneros JM, Bouma BE, Bressner J, Halpern EF, Shishkov M, Lauwers GY, Mino-Kenudson M, Nishioka NS, Tearney GJ. Optical coherence tomography to identify intramucosal carcinoma and high-grade dysplasia in Barrett's esophagus. *Clin Gastroenterol Hepatol* 2006; **4**: 38-43 [PMID: 16431303 DOI: 10.1016/S1542-3565(05)00746-9]

46 **Hsiung PL**, Phatak DR, Chen Y, Aguirre AD, Fujimoto JG, Connolly JL. Benign and malignant lesions in the human breast depicted with ultrahigh resolution and three-dimensional optical coherence tomography. *Radiology* 2007; **244**: 865-874 [PMID: 17630358 DOI: 10.1148/radiol.2443061536]

47 **Wong BJ**, Jackson RP, Guo S, Ridgway JM, Mahmood U, Su J, Shibuya TY, Crumley RL, Gu M, Armstrong WB, Chen Z. In vivo optical coherence tomography of the human larynx: normative and benign pathology in 82 patients. *Laryngoscope* 2005; **115**: 1904-1911 [PMID: 16319597 DOI: 10.1097/01.MLG.0000181465.17744.BE]

48 **Ridgway JM**, Ahuja G, Guo S, Su J, Mahmood U, Chen Z, Wong B. Imaging of the pediatric airway using optical coherence tomography. *Laryngoscope* 2007; **117**: 2206-2212 [PMID: 18322424 DOI: 10.1097/MLG.0b013e318145b306]

49 **Davoudi B**, Lindenmaier A, Standish BA, Allo G, Bizheva K, Vitkin A. Noninvasive in vivo structural and vascular imaging of human oral tissues with spectral domain optical coherence tomography. *Biomed Opt Express* 2012; **3**: 826-839 [PMID: 22567578 DOI: 10.1364/BOE.3.000826]

50 **Carlos RC**, Scheiman JM, Hussain HK, Song JH, Francis IR, Fendrick AM. Making cost-effectiveness analyses clinically relevant: the effect of provider expertise and biliary disease prevalence on the economic comparison of alternative diagnostic strategies. *Acad Radiol* 2003; **10**: 620-630 [PMID: 12809415]

51 **Scheiman JM**, Carlos RC, Barnett JL, Elta GH, Nostrant TT, Chey WD, Francis IR, Nandi PS. Can endoscopic ultrasound or magnetic resonance cholangiopancreatography replace ERCP in patients with suspected biliary disease? A prospective trial and cost analysis. *Am J Gastroenterol* 2001; **96**: 2900-2904 [PMID: 11693324 DOI: 10.1016/S0002-9270(01)02807-6]

52 **Snady H**, Cooperman A, Siegel J. Endoscopic ultrasonography compared with computed tomography with ERCP in patients with obstructive jaundice or small peri-pancreatic mass. *Gastrointest Endosc* 1992; **38**: 27-34 [PMID: 1612375 DOI: 10.1016/S0016-5107(92)70326-5]

53 **Rösch T**, Hofrichter K, Frimberger E, Meining A, Born P, Weigert N, Allescher HD, Classen M, Barbur M, Schenck U, Werner M. ERCP or EUS for tissue diagnosis of biliary strictures? A prospective comparative study. *Gastrointest Endosc* 2004; **60**: 390-396 [PMID: 15332029 DOI: 10.1016/S0016-5107(04)01732-8]

54 **Domagk D**, Poremba C, Dietl KH, Senninger N, Heinecke A, Domschke W, Menzel J. Endoscopic transpapillary biopsies and intraductal ultrasonography in the diagnostics of bile

duct strictures: a prospective study. *Gut* 2002; **51**: 240-244 [PMID: 12117887 DOI: 10.1136/gut.51.2.240]
55 **Testoni PA**, Mangiavillano B, Mariani A. Optical coherence tomography for investigation of the pancreatico-biliary system: still experimental? *JOP* 2007; **8**: 156-165 [PMID: 17356238]
56 **Tearney GJ**, Brezinski ME, Southern JF, Bouma BE, Boppart SA, Fujimoto JG. Optical biopsy in human pancreatobiliary tissue using optical coherence tomography. *Dig Dis Sci* 1998; **43**: 1193-1199 [PMID: 9635607]
57 **Tearney GJ**, Brezinski ME, Southern JF, Bouma BE, Boppart SA, Fujimoto JG. Optical biopsy in human pancreatobiliary tissue using optical coherence tomography. *Dig Dis Sci* 1998; **43**: 1193-1199 [PMID: 9635607 DOI: 10.1023/A:1018891304453]
58 **Testoni PA**, Mariani A, Mangiavillano B, Albarello L, Arcidiacono PG, Masci E, Doglioni C. Main pancreatic duct, common bile duct and sphincter of Oddi structure visualized by optical coherence tomography: An ex vivo study compared with histology. *Dig Liver Dis* 2006; **38**: 409-414 [PMID: 16584931 DOI: 10.1016/j.dld.2006.02.014]
59 **Testoni PA**, Mangiavillano B, Albarello L, Mariani A, Arcidiacono PG, Masci E, Doglioni C. Optical coherence tomography compared with histology of the main pancreatic duct structure in normal and pathological conditions: an 'ex vivo study'. *Dig Liver Dis* 2006; **38**: 688-695 [PMID: 16807151 DOI: 10.1016/j.dld.2006.05.019]
60 **Testoni PA**, Mangiavillano B, Albarello L, Arcidiacono PG, Mariani A, Masci E, Doglioni C. Optical coherence tomography to detect epithelial lesions of the main pancreatic duct: an Ex Vivo study. *Am J Gastroenterol* 2005; **100**: 2777-2783 [PMID: 16393235 DOI: 10.1111/j.1572-0241.2005.00326.x]
61 **Singh P**, Chak A, Willis JE, Rollins A, Sivak MV. In vivo optical coherence tomography imaging of the pancreatic and biliary ductal system. *Gastrointest Endosc* 2005; **62**: 970-974 [PMID: 16301046 DOI: 10.1016/j.gie.2005.06.054]
62 **Testoni PA**, Mariani A, Mangiavillano B, Arcidiacono PG, Di Pietro S, Masci E. Intraductal optical coherence tomography for investigating main pancreatic duct strictures. *Am J Gastroenterol* 2007; **102**: 269-274 [PMID: 17100970 DOI: 10.1111/j.1572-0241.2006.00940.x]
63 **Hwang JH**, Cobb MJ, Kimmey MB, Li X. Optical coherence tomography imaging of the pancreas: a needle-based approach. *Clin Gastroenterol Hepatol* 2005; **3**: S49-S52 [PMID: 16012997 DOI: 10.1016/S1542-3565(05)00259-4]
64 **Seitz U**, Freund J, Jaeckle S, Feldchtein F, Bohnacker S, Thonke F, Gladkova N, Brand B, Schröder S, Soehendra N. First in vivo optical coherence tomography in the human bile duct. *Endoscopy* 2001; **33**: 1018-1021 [PMID: 11740643 DOI: 10.1055/s-2001-18934]
65 **Poneros JM**, Tearney GJ, Shiskov M, Kelsey PB, Lauwers GY, Nishioka NS, Bouma BE. Optical coherence tomography of the biliary tree during ERCP. *Gastrointest Endosc* 2002; **55**: 84-88 [PMID: 11756925 DOI: 10.1067/mge.2002.120098]
66 **Testoni PA**, Mangiavillano B. Optical coherence tomography in detection of dysplasia and cancer of the gastrointestinal tract and bilio-pancreatic ductal system. *World J Gastroenterol* 2008; **14**: 6444-6452 [PMID: 19030194 DOI: 10.3748/wjg.14.6444]
67 **Mangiavillano B**, Mariani A A, Petrone MC. An intrapancreatic cholangiocarcinoma detected with optical coherence tomography during endoscopic retrograde cholangiopancreatography. *Clin Gastroenterol Hepatol* 2008; **6**: A30 [PMID: 18407794 DOI: 10.1016/j.cgh.2008.02.004]
68 **Cizginer S,** Deshpande V, Iftimia N, Karaca C, Brugge WR. Optical Coherence Tomography (OCT) Imaging Can Detect Fine Morphologic Features of Pancreatic Cystic Neoplasms and Differentiate Between Mucinous and Non-Mucinous Cysts. *Gastroenterol* 2009; **136**: 45 [DOI: 10.1016/S0016-5085(09)60204-3]
69 **Iftimia N**, Cizginer S, Deshpande V, Pitman M, Tatli S, Iftimia NA, Hammer DX, Mujat M, Ustun T, Ferguson RD, Brugge WR. Differentiation of pancreatic cysts with optical coherence tomography (OCT) imaging: an ex vivo pilot study. *Biomed Opt Express* 2011; **2**: 2372-2382 [PMID: 21833374 DOI: 10.1364/BOE.2.002372]

P- Reviewers: Triantafyllou K, Tham TCK **S- Editor**: Qi Y
L- Editor: A **E- Editor**: Wu HL

百世登
Baishideng®

Published by **Baishideng Publishing Group Co., Limited**
Flat C, 23/F., Lucky Plaza,
315-321 Lockhart Road, Wan Chai, Hong Kong, China
Fax: +852-65557188
Telephone: +852-31779906
E-mail: bpgoffice@wjgnet.com
http://www.wjgnet.com